

A *p*-*tert*-butylcalix[6]arene bearing phosphinoyl pendant arms for the complexation and sensitisation of lanthanide ions †

Flor de María Ramírez,^{a,b} Sabi Varbanov,^{a,c} Corine Cécile,^a Gilles Muller,^a Nicolas Fatin-Rouge,^a Rosario Scopelliti^a and Jean-Claude G. Bünzli^{*a}

^a Institute of Molecular and Biological Chemistry, BCH 1402, Swiss Federal Institute of Technology, CH-1015 Lausanne, Switzerland. E-mail: jean-claude.bunzli@epfl.ch

^b Instituto Nacional de Investigaciones Nucleares, Departamento de Química, Km 36.5 Carretera México-Toluca, Salazar, Municipio de Ocoyoacac, C.P. 52045, Edo. de México, México

^c Institute of Polymers, Bulgarian Academy of Sciences, BG-1113 Sofia, Bulgaria

Received 27th June 2002, Accepted 24th September 2002

First published as an Advance Article on the web 28th October 2002

The new lower rim functionalised macrocycle 5,11,17,23,29,35-hexa-*tert*-butyl-37,38,39,40,41,42-hexakis(dimethylphosphinoylmethoxy)calix[6]arene (B_6bL^6) has been synthesised. Temperature dependent 1H and ^{31}P NMR studies indicate a mixture of conformers with a time-averaged C_{6v} symmetry at 405 K in dmsd- d_6 ; ΔG^\ddagger values for conformational interconversion processes are equal to 68(1) and 75(2) kJ mol $^{-1}$ and reveal a semi-flexible macrocycle with alternate *in-out* cone conformation, a fact confirmed by molecular mechanics and dynamics calculations. B_6bL^6 crystallises as a dimer where the two calixarenes are linked through hydrogen bonding and surrounded by water and toluene molecules in the lattice. UV-Vis spectrophotometric titration of B_6bL^6 with La(III) in acetonitrile yields stability constants $\log \beta_1 = 9.8$ and $\log \beta_2 = 19.6$ for the 1 : 1 and 1 : 2 ($Ln : B_6bL^6$) species, respectively. The corresponding complexes with La, Eu, Gd and Tb have been isolated and characterised. Lifetime determinations of the Eu(III) and Tb(III) complexes in acetonitrile solution are consistent with no or little interaction of water molecules in the inner co-ordination sphere. The new ligand sensitises reasonably well the luminescence of the Tb(III) ($Q_{abs} = 4.8\%$, $\tau_f = 2.1$ ms, 1 : 1 complex) and Eu(III) ($Q_{abs} = 2.5\%$, $\tau = 2.0$ ms, 1 : 2 complex) ions.

Introduction

The impact of calixarenes in supramolecular chemistry¹ derives from their easy functionalisation on both the wide and narrow rims, resulting in a large versatility.¹ Specific functionalities can be implemented in the macrocyclic receptors by changing the diameter or the depth of the cavity, the substituents grafted onto the rims or by modifying the polarity of the cavity. Receptors fitted with phosphorous-containing pendant arms form a special class of calixarenes.² They are used to design chemical sensors,³ catalysts,⁴ or selective electrodes for heavy metal ions,⁵ but their main applications lie in separation sciences^{1,2,6} since they easily form complexes with all metal ions, including 4f- and 5f-ions. The nuclear industry is particularly interested in phosphorous-organic derivatives for the extraction of the main radioactive contaminants from wastes before their confinement.⁷ Good results in the de-categorisation of nuclear wastes have been achieved using calix[*n*]arene phosphine oxides ($n = 4-8$) which extract Eu(III), Th(IV), Pu(IV) and Am(III) with high efficiency.^{8,9} The functionalised position, the size of calixarenes, as well as the nature of the alkyl groups on the phosphoryl functions influence the efficiency of the extraction.⁶ The best extractants for the Am(III) and Np(III) ions are calixarenes substituted in the wider rim by CMPO arms [CMPO = *N,N*-diisobutylcarbamoylmethyl)octylphenyl-

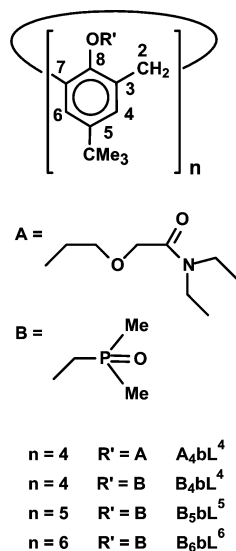
phosphine oxide], while substitution on the narrow rim results in better extraction of Th(IV) over Eu(III).⁹

Our interest for lanthanide complexes with calixarenes lies in the development of model molecules for the study of energy transfer processes and magnetic interactions¹⁰ as well as in the engineering of functionalised receptors for the design of luminescent probes and extraction systems. With respect to the latter, our research program has focused on calixarenes bearing either ether amide¹¹ or phosphinoyl¹² groups. In previous papers we have reported on the interaction between A_4bL^4 , a *p*-*tert*-butylcalix[4]arene substituted at the narrow rim with ether-amide pendant arms (Scheme 1). This macrocycle was shown to act as an inorganic-organic receptor, encapsulating both a lanthanide ion and a solvent molecule. In addition, the coordination cavity for the Ln(III) ion is tightened by a water molecule hydrogen bonded to the phenolic oxygen atoms and rigidifying it, so that the calixarene behaves as a good sensitiser of the Tb(III) luminescence.¹¹ Replacing the ether-amide substituents by dimethylphosphinoylmethylene pendant arms leads to B_4bL^4 (Scheme 1), which interacts more strongly with Ln(III) ions, forming both 1 : 1 and 1 : 2 complexes in acetonitrile; in this case, solvent composition strongly influences the solvation state of the macrocyclic edifices.¹²

Calix[6]arenes are more flexible than the smaller calix[4]arenes and may lead to interesting extended structures (*e.g.* channel-like)¹³ so that we turn here to a new narrow-rim substituted *p*-*tert*-butylcalix[6]arene, 5,11,17,23,29,35-hexa-*tert*-butyl-37,38,39,40,41,42-hexakis(dimethylphosphinoylmethoxy)calix[6]arene, B_6bL^6 (Scheme 1). We report its synthesis and structural properties both in the solid state, based on X-ray diffraction data, and in solution where a conformational study is carried out by NMR measurements and interpreted by

† This paper is dedicated to the memory of Professor Luigi M. Venanzi.

Electronic supplementary information (ESI) available: torsion angles in B_6bL^6 (Fig. S1), absorption spectra of the ligand and its La^{III} complexes (Fig. S2), NMR spectra of the La(III) complexes (Figs. S3, S4), high resolution luminescence spectra of the Eu(III) complexes (Fig. S5), emission spectra of the Tb(III) complexes (Fig. S6). See <http://www.rsc.org/suppdata/dt/b2/b206238k/>



Scheme 1

molecular mechanics and molecular dynamics calculations. Furthermore, its coordination behaviour towards lanthanide ions and its ability to sensitise their luminescence is investigated and discussed.

Results and discussion

Synthesis and structural characterisation of B_6bL^6

The ligand B_6bL^6 was prepared in 43% yield *via* a Williamson reaction¹² by refluxing the hexasodium derivative of *p*-*tert*-butylcalix[6]arene and chloro(dimethylphosphinoyl)methane in toluene. The prepared B_6bL^6 is a white hygroscopic powder with composition $B_6bL^6 \cdot 4H_2O$ as indicated by elemental analysis. The vibrational spectrum displays a very intense and sharp $\nu(P=O)$ band at 1164 cm^{-1} , which shifts to $1178\text{--}1180\text{ cm}^{-1}$ after heating the KBr pellet at 393 K for 24–36 h, as a consequence of the removal of water trapped by the phosphinoyl groups. The hygroscopic nature of B_6bL^6 is indeed consistent with the known affinity of the phosphoryl groups for water molecules.¹⁴ The elevated temperature needed for a complete removal of water suggests the formation of $HOH \cdots O=P$ hydrogen bonds rather than an interaction with the phenolic oxygen atoms. Intermolecular hydrogen bonding is, however, also feasible, as suggested by the formation of an aqueous–organic emulsion during the water work up of the ligand in methylene chloride; this ‘interphase’ contains more than 98% of the phosphinoyl-*p*-*tert*-butylcalix[6]arene which can only be laboriously recovered as a powdered sample. The peculiar conformational flexibility of B_6bL^6 leaves the P=O groups exposed to the aqueous environment, thus intermolecular hydrogen bonding interactions occur and semi-oligomers are produced which form an emulsion with methylene chloride. Such a phenomenon was not observed with the corresponding derivatives of *p*-*tert*-butylcalix[*n*]arenes^{12,15} (B_4bL^4 and B_5bL^5).

The chemical structure of B_6bL^6 is confirmed by 1H , $^{13}C\{^1H\}$ and $^{31}P\{^1H\}$ NMR spectra measured in $d_6\text{-}DMSO$. At temperatures higher than 378 K, 1H NMR signals for all the protons appear as singlets, except for P-CH₂ and P-Me₂ which appear as doublets at 405 K as a result of the coupling with ^{31}P (Fig. 1).^{2,16} At 405 K, the H₂O resonance appears at 2.68 ppm and shifts downfield to 3.3 ppm at 293 K, which allows its unambiguous assignment.¹⁷ A single sharp peak is seen at +35.82 (against 85% H₃PO₄ in the $^{31}P\{^1H\}$ NMR spectrum at 378 K), this value being typical for a tertiary phosphine oxide group with two methyl groups and one methylene moiety bonded to the phosphorus atom.¹⁶ These data are consistent

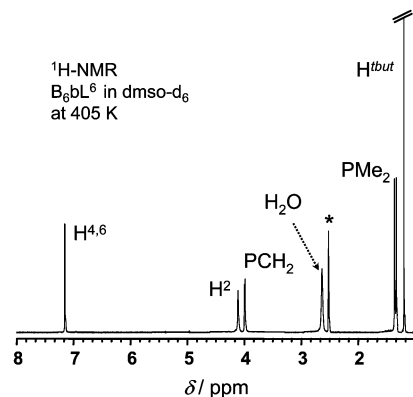


Fig. 1 1H NMR spectrum of B_6bL^6 in $d_6\text{-}DMSO$ at 405 K; the star denotes the solvent peak.

with an averaged molecular symmetry C_{6v} in $d_6\text{-}DMSO$ at $T > 378\text{ K}$.

Conformational interconversion processes of B_6bL^6 in solution

The conformations adopted by large flexible calixarenes depend on the ring size, the substituents on the rims and the polarity of the solvent.¹ Calix[6]arenes can exist under eight ‘up-down’ conformations (with respect to the phenyl rings) and the flexibility of the large annulus allows other conformations in which, for instance, one or more aryl rings lie approximately in the average plane of the molecule.¹⁶ Substituents at the narrow and wide rims influence the conformational equilibria and lead to ‘pinched’ conformers.¹⁸ Two pathways are potentially available for the conformational ring interconversion: one in which the OR substituents swing through the annulus and another one involving a motion of the *para* substituents through the annulus, even if these substituents are relatively bulky such as *p*-*tert*-butyl groups.¹⁹ At room temperature, the NMR spectra of B_6bL^6 in various solvents ($d_6\text{-}DMSO$, CD_3CN , $CDCl_3$, and CD_2Cl_2) are different and quite complex, suggesting the presence of a mixture of mobile conformers, the proportion of which is influenced by the nature of the solvent, as previously observed.²⁰ To gain an insight into the conformational interconversion processes of B_6bL^6 , we have measured its temperature-dependent ^{31}P and 1H NMR spectra in the ranges 223–333 K ($CDCl_3$, Fig. 2) and 293–405 K ($d_6\text{-}DMSO$).

At low temperatures (<233 K), the 1H and, partially, the $^{31}P\{^1H\}$ spectra are broadened, pointing to interchange processes between several conformers. Indeed, the ^{31}P spectrum displays a wealth of signals, two of them being quite sharp (39.8 and 46.8 ppm), while at least four sets of *tert*-butyl resonances can be identified on the 1H spectrum (not shown on Fig. 2). We tentatively assign the two ^{31}P signals at 46.8 and 39.8 ppm to in and out positions, relative to the calixarene cavity, of the *ortho* substituents of a low energy conformer. Molecular modelling (see below) clearly shows that the conformation extracted from X-ray measurements is existing at low temperature in solution. Upon increasing the temperature to 263 K, the P-CH₂ resonances sharpen and several well resolved doublets are seen in the range 3–5 ppm (methylene groups). In particular, the outer portions of the multiplet around 3.5 and 4.7 ppm feature two pairs of doublets (Ar-CH₂-Ar) corresponding to two different conformations. The central part of the multiplet is more difficult to interpret since it also contains signals from the P-CH₂ methylene groups. In the ^{31}P spectrum, the intensity of the two sharp resonances seen at 223 K diminishes, the broadened singlet at 43.2 ppm (223 K) shifts to 41 ppm and gains in intensity and the other resonances coalesce into two very broad features. Raising the temperature to 303 K causes a further decrease of the two sharp ^{31}P peaks which move towards high field and broaden, but their chemical shift difference remains constant and three other relatively broad

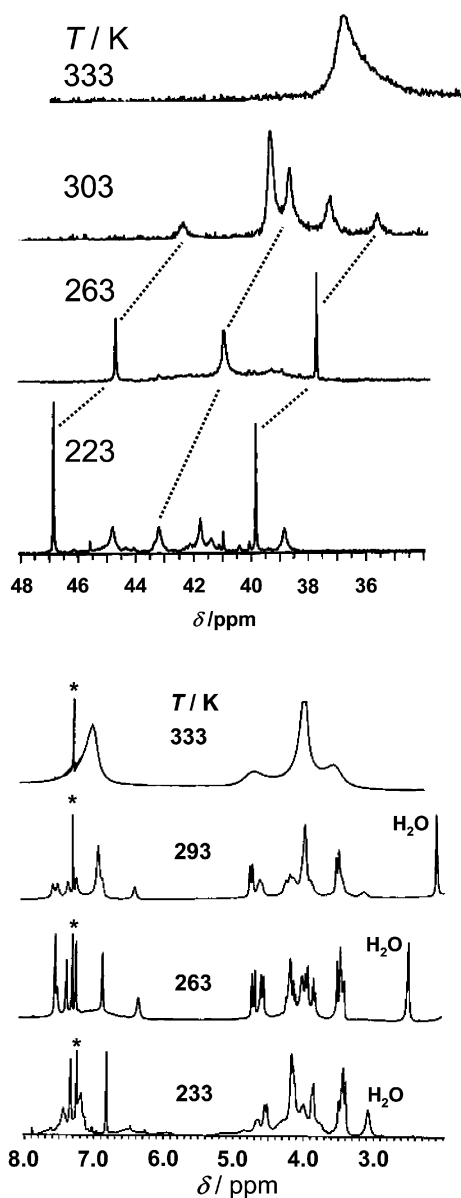


Fig. 2 Temperature-dependent $^{31}\text{P}\{^1\text{H}\}$ - (top) and ^1H - (bottom) NMR spectra of B_6bL^6 in CDCl_3 ; the stars denote solvent peaks.

resonances are identified. Coalescence is reached at 333 K. The two broad methylene resonances at 3.55 and 4.7 ppm ($\text{P}-\text{CH}_2$) are assigned as arising from the interconversion between pinched conformers. At low temperature, it is expected that pinched conformers are in equilibrium with the alternate *in-out* conformation depicted in Fig. 3. The free energy barrier for this process has been estimated using the Eyring equation applied to the rate constants extracted from the temperature dependence of the sets of methylene resonances ($\text{Ar}-\text{CH}_2-\text{Ar}$) and the coalescence temperature T_c .²¹

$$k_c = \pi \times \sqrt{\frac{\Delta\nu^2 + 6J^2}{2}}$$

where $\Delta\nu$ is the chemical shift difference between the centres of the two doublets and J the coupling constant. ΔG^\ddagger values amount to 68 ± 1 and 62 ± 1 kJ mol^{-1} in dmsd-d_6 and CDCl_3 , respectively. Upon increasing the temperature further, an additional coalescence is detected at 378 K in dmsd-d_6 with a single peak resonance for the bridging methylene protons between the phenyl rings (Fig. 1). This process is interpreted as the macrocyclic ring interconversion because its free energy of

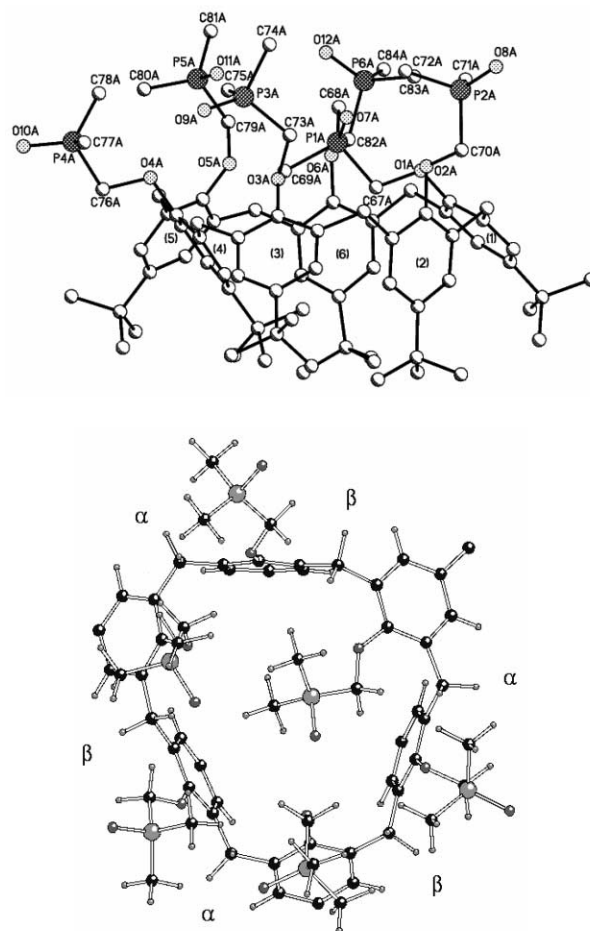


Fig. 3 Structure of B_6bL^6 : (top) X-ray structure of molecule A with the partial atom-numbering scheme; (bottom) result of the molecular mechanics modelling.

activation (75 ± 1.5 kJ mol^{-1}) is larger than that required for interconversion between pinched conformers. The 7 kJ mol^{-1} difference observed between the two free energies of interconversion can be related to the bulkiness of the phosphinoyl arm, because unsubstituted calix[6]arenes do not display any difference in free energy of activation between these two processes. The ΔG^\ddagger values observed for B_6bL^6 are large and effectively point to the flexibility of the *p-tert*-calix[6]arene ring being curtailed by the dimethylphosphinoylmethoxy substitution at the narrow rim. As a comparison, free energies of activation in the range 54–57 kJ mol^{-1} are reported for the conformational inversion of *p-alkyl*calix[6]arenes (alkyl = H, allyl, *tert*-butyl, *tert*-octyl), in chloroform, with coalescence temperatures between 271 and 285 K (at 100 MHz).^{1e} On the other hand, the corresponding value reported for a narrow-rim monosubstituted *p-tert*-butylcalixarene with a benzyl group is 65 kJ mol^{-1} in dmsd-d_6 ($T_c = 320$ K at 300 MHz); when the benzyl moiety bears *para* substituents, ΔG^\ddagger becomes much larger (>70 kJ mol^{-1}).²² Finally, phosphate monosubstitution of calix[6]arene has been shown to considerably rigidify the skeleton of the macrocycle, with ΔG^\ddagger values for ring interconversion ranging between 67 and 87 kJ mol^{-1} . On the other hand, the activation barrier for pinched conformer interconversion of mono- and di-substituted phosphorylated calix[6]arenes is much lower, between 44 and 55 kJ mol^{-1} .¹⁸ We therefore conclude that conformational interconversion of the macrocyclic ring of B_6bL^6 occurs *via* the movement of the dimethylphosphinoylmethoxy substituents of the lower rim through the annulus. The free energy required for the process involving the upper rim is indeed reported to be larger than 88 kJ mol^{-1} .¹⁸ According to the classification of

Kanamathareddy and Gutsche,¹⁹ B₆bL⁶ has consequently a semi-mobile structure in solution.

The H₂O resonance moves slowly from high field to low field as the temperature is increased; its location at room temperature indicates a very weak interaction with the ligand. Together with the activation barrier reported above, this points to an absence of water molecules in the cavity of the calixarene since H- π interaction or intramolecular hydrogen bonding formed by the phosphinoyl-HOH-calixarene cavity would be reflected in the ¹H NMR spectra and the ΔG^\ddagger value.

Crystal and molecular structure of B₆bL⁶·13H₂O·0.5C₇H₈

Crystals are monoclinic and the asymmetric unit contains a pair of independent molecules [labelled A (Fig. 3) and B] related by a pseudo twofold axis and linked together by hydrogen bonds between water molecules and phosphinoyl groups (Fig. 4). Each calixarene molecule is surrounded by 13 water

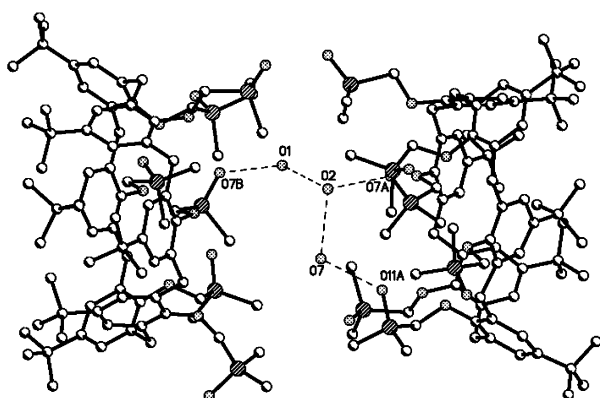


Fig. 4 Hydrogen bond network connecting two molecules of B₆bL⁶.

molecules and a half toluene molecule. Fig. 3 displays a partial atom-numbering scheme for molecule A, while conformational angles are reported in Table 1. The macrocycle forms a kind of triangle with three of the phenyl rings at the vertex and the other three along the sides of the triangle. Adjacent phenyl rings are almost perpendicular, as shown by their dihedral angles, while rings 1 and 4 are almost parallel, their dihedral angles being quite small. The conformation can be described as being a distorted alternate *in-out* cone conformation (u,u,u,u,u,u).¹⁹ However, the structure may also be seen as comprised of four phenyl rings (2, 3, 5 and 6) forming a kind of calix[4]arene with the two additional aromatic rings (1, 4) positioning themselves between the two halves of the calix[4]arene. It is noteworthy that the phosphinoyl substituent on ring 1 points inside the cavity while its counterpart on ring 4 extends outward, in the prolongation of the phenyl ring plane. The arms on rings 2 and 6 also completely point outside, to make room for substituent 1, while only the P(O)Me₂ part of the remaining two arms are located outside the cone.

Water molecules play a fundamental role in the structure since they are involved in a complex network of hydrogen bonds (Table 2). They link the molecules to form the dimers (Fig. 4) and are probably responsible for the peculiar positioning of the phosphinoyl arms, which is unusual for a calix[6]arene.¹ There are two kinds of hydrogen bonds: those involving the P=O groups (e.g. O10B...O6 = 2.611(12) Å; O12B...O8 = 2.509(18) Å) and those between water molecules themselves. The toluene molecule is located near the *tert*-butyl groups of molecule A but lies completely outside the cavity.

Molecular mechanics and dynamics calculations

In the past, such theoretical calculations have contributed to a better understanding of the conformation adopted by parent

Table 1 Dihedral angles (ϕ and ϕ') between phenyl rings in the molecular structure of B₆bL⁶ (for the numbering, see Fig. 3) as determined from X-ray diffraction data and modelling calculations (see text)

Rings	X-Ray diffraction (molecule A)		Modelling	
	ϕ°	ϕ'°	ϕ°	ϕ'°
1–2	78.8	–131.3	79	–140.7
2–3	155.6	–98.2	141.6	–80.1
3–4	71.1	–154.3	75.9	–140.3
4–5	178.7	–93.3	170.9	–110.4
5–6	75.4	–118.7	67.9	–123.1
6–1	166.6	–106.0	158.1	–92.8

Table 2 Main hydrogen interactions involving the P=O moieties in the dimer of B₆bL^{6a}

	O...O/Å	P=O...O/°
O7A...O2	2.769(11)	121.3(4)
O7B...O1	2.689(11)	123.3(4)
O8A...O21	2.59(3)	136.8(9)
O8A...O23	2.83(3)	151.9(8)
O9A...O4	2.759(11)	116.5(5)
O9B...O20A	2.82(3)	113.9(6)
O9B...O10	2.851(13)	119.9(5)
O10A...O22C	2.74(2)	142.1(7)
O10B...O6	2.611(12)	123.8(5)
O11A...O7	2.874(15)	120.3(5)
O11B...O4A	2.699(12)	121.9(5)
O12A...O12	2.74(2)	115.0(5)
O12B...O8	2.509(18)	126.1(8)

^a Hydrogen atoms were not located for water molecules; the analysis therefore relies only on the O...O contacts.

calix[*n*]arenes.²³ For instance, *pinched cone*^{1,24} or *winged* conformations for calix[6]arene have been predicted by calculations,^{1,2,6,23} while similar conformations have been observed in solution.^{1,23–25} In an attempt to identify the lowest energy conformation of B₆bL⁶, we have performed calculations without packing forces or intermolecular interactions. The structure was refined in vacuum at 0 K after molecular dynamics calculations using the following sequence: heating to 1000, 600, 400 K for 5 ps each. For the estimation of the torsion angles ϕ (C1A–C6A–C7A–C9A) and ϕ' (C6A–C7A–C9A–C8A), defining the orientation of one phenyl ring relative to the next one, on a fragment of the molecule comprised of two phenyl units only, the fragment was kept at these elevated temperatures to allow for the reorganisation of the phosphinoyl arms only (Fig. S1, ESI†). Finally, a new sequence was applied without constraint, heating to 300 K for 50 ps, with dynamic time steps of 0.5 fs. Then, the structure with the lowest energy obtained during the previous procedure was singled out and its energy minimized. The potential energy for the calculated structure of the calix[6]arene, applying the Dreiding force field 2.21, is 1045 kJ mol^{–1}. The calculations confirm the conformation obtained from X-ray analysis for the most stable alternate *in-out* cone conformer (Fig. 3, Table 1). This conformer can be characterised by two sets of ϕ and ϕ' angles, denoted α and β . Interestingly, the average α and β pairs of angles calculated from X-ray data are very close to those predicted by the modelling process (Table 3). Additionally, the values obtained for the fragment comprised of two phenyl units only compare reasonably well with the experimental data. This points to the alternate *in-out* conformation being stable with weak constraints resulting from the cyclisation of the hexamer B₆bL⁶ as compared with other potential steric hindrances.

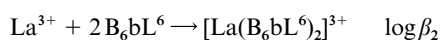
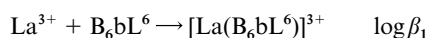
Complexation of B₆bL⁶ with lanthanide ions

The interaction between B₆bL⁶ and La(III) has been probed by spectrophotometric titration of the ligand (1.7×10^{-4} M) by

Table 3 Mean torsion angles $\langle\phi\rangle$ and $\langle\phi'\rangle$ ($^\circ$) of the connecting methylene moieties in the X-ray structure of B_6bL^6 , in the structure minimized by molecular modelling and in the fragment containing two phenyl rings only

Pair of dihedral angles	Mean angle/ $^\circ$					
	X-Ray diffraction (molecule A)		Calculations		Fragment (calc.)	
	$\langle\phi\rangle$	$\langle\phi'\rangle$	$\langle\phi\rangle$	$\langle\phi'\rangle$	ϕ	ϕ'
α	75.1	-134.8	74.5	-134.5	63.7	-138.7
β	167.0	-99.2	157	-94.5	143.7	-70.7

2.4×10^{-4} M $La(ClO_4)_4 \cdot 4.5H_2O$ in degassed and anhydrous acetonitrile and up to a ratio $R = [La(III)]/[B_6bL^6] = 4$. Factor analysis revealed three absorbing species and data could be satisfactorily fitted to the following model:



with $\log\beta_1 = 9.8 \pm 0.9$ and $\log\beta_2 = 19.6 \pm 1.9$. The latter reproduce reasonably well the experimental absorption spectra (Fig. S2, ESI†). However since the spectra of the complexes are heavily correlated, these data should be taken with care. The stability of the complexes is close to that found for complexes with B_4bL^4 ($\log\beta_1 = 11.4$, $\log\beta_2 = 19.6$).¹² The somewhat smaller stability constant found for the 1 : 1 complex with B_6bL^6 results from a smaller degree of preorganisation of the ligand which exists as an equilibrium between several conformations under the experimental conditions used while only one conformer is revealed by ^{13}P and 1H NMR for B_4bL^4 .¹²

The 1H and $^{31}P\{^1H\}$ NMR spectra [$Ln(III) = La, Eu$] recorded at variable temperature in dried and degassed CD_3CN and $dmsO-d_6$ change substantially depending on the ligand-to-metal ratio (Fig. S3, ESI†), but since several conformational isomers with low symmetry are present, detailed interpretation proved impracticable because coalescence could not be reached, as a result of the ligand conformations becoming more the rigid upon complexation. For instance, careful integration of the 1H NMR spectrum at 229 K reveals the presence of at least four isomers (Fig S4, ESI†). The influence of the $Ln(III)$ cation on the flexibility of the ligand is similar to that observed when calix[6]arene is functionalised with large arms or is partially O-substituted.^{18,26}

That complexes with two different stoichiometries form is substantiated by the isolation of the corresponding hygroscopic complexes $[Ln(B_6bL^6)](ClO_4)_3 \cdot nH_2O$ ($n = 3$, $Ln = La, 1$; $n = 6$, $Ln = Eu, 2$, $Gd, 3$, and $Tb, 4$) and $[Ln(B_6bL^6)_2](ClO_4)_3 \cdot nH_2O$ ($n = 3$, $Ln = La, 5$, $Eu, 6$; $n = 5$, $Ln = Gd, 7$; $n = 4$, $Ln = Tb, 8$). Vibrational spectra clearly show the characteristic absorptions of ionic perchlorate around 624 and 1100 cm^{-1} for both stoichiometries. On the other hand, absorption bands arising from co-ordinated perchlorate anions are also visible in the ranges 630–640 and 1120–1150 cm^{-1} . For instance, the bands at 635 and 1140 cm^{-1} in the spectra of the 1 : 1 complexes can be interpreted as reflecting the presence of bidentate perchlorate anions.²⁷ A more detailed analysis is not possible due to the overlap with the ligand P=O stretching vibrations. After drying the pellets during 24 h at 393 K, the spectra become more resolved, especially in the case of the 1 : 2 complexes. The P=O band is usually split upon complexation and is red-shifted.¹² Here we observe only one component, slightly blue-shifted (7–11 and 4–11 cm^{-1} for 1 : 1 and 1 : 2 complexes, respectively), so that we infer that the other constituent lies in the broad feature extending from 1050 to 1150 cm^{-1} . Water is completely removed from the complexes after heating the KBr pellets, which means that the interaction with the metal ion and/or the calixarene is relatively weak. No single crystals could be

obtained to characterise further the structure of the isolated complexes.

Photophysical properties

In acetonitrile, B_6bL^6 displays one large absorption band around 48800 cm^{-1} assigned to a transition mainly located on the phosphinoyl group and a less intense split band at 37880 and 36900 cm^{-1} assigned to transitions mainly located on the phenyl rings. Upon complexation, the latter undergo a bathochromic shift of about 700–900 cm^{-1} ; the molar absorption coefficients for the 1 : 1 complexes are 20–50% smaller than those of B_6bL^6 , while they are about 50% larger for the 1 : 2 complexes, reflecting large changes in the ligand complexation behaviour upon stoichiometry change (Table 4). In the solid state, the ligand $^* \pi \leftarrow \pi$ (phenyl) bands are red shifted 1300 and 900 cm^{-1} while transitions for the complexes occur approximately at the same energy. Excitation at 35970 cm^{-1} of solid state samples cooled to 77 K leads to the observation of two emission bands for the ligand arising from a singlet state located at 33080 cm^{-1} and a triplet state at 22870 cm^{-1} . Complexation with $La(III)$ induces a red shift of 1850 and 2520 cm^{-1} , respectively, in the case of the 1 : 1 complex; the shift is much smaller for the 1 : 2 complex: 830 and 1800 cm^{-1} , respectively (Fig. 5). The triplet state is located conveniently to potentially

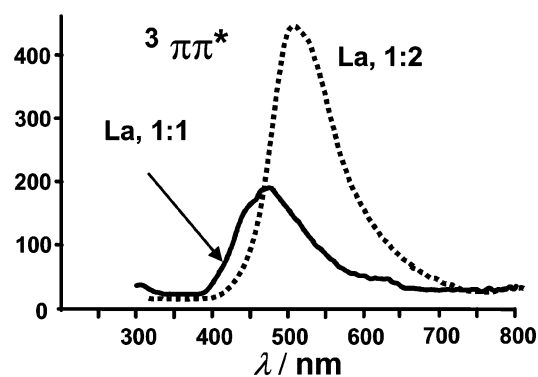


Fig. 5 Phosphorescence spectra of powdered samples of the $La(III)$ 1 : 1 and 1 : 2 complexes with B_6bL^6 at 77 K.

transfer energy onto the $^5D_0(Eu)$ and $^5D_4(Tb)$ levels,²⁸ and indeed 1 : 1 complexes of these ions only display metal-centred luminescence; a similar situation prevails for the 1 : 2 complex with Eu , but a weak $^3 \pi \pi^*$ emission is still seen on the spectrum of the 1 : 2 Tb compound.

To gain additional information on the chemical environment of the $Eu(III)$ ions, we turned to high resolution emission and excitation spectra. Upon ligand excitation, the emission spectra of both 1 : 1 and 1 : 2 complexes (powdered samples, 20 K, Fig. S5, ESI†) are dominated by the electric dipole $^5D_0 \rightarrow ^7F_2$ transition; the relative integrated intensities of the $^5D_0 \rightarrow ^7F_J$ transitions are: 0.80, 1.00, 9.1, 0.2 and 1.1 (1 : 1 complex) and 0.6, 1.00, 8.0, 0.2 and 1.1 (1 : 2 complex) for $J = 0, 1, 2, 3$ and 4, respectively. The bands are relatively broad, with maximum splitting with respect to ligand field effects. The $^5D_0 \rightarrow ^7F_0$

Table 4 Energy of the $^*π←π(\text{phenyl})$ transitions (cm^{-1})^a of B_6bL^6 and its complexes in acetonitrile, of the $^1ππ^*$ and $^3ππ^*$ states in the solid state at 77 K (solid state samples), and $^3ππ^*$ state lifetime (frozen acetonitrile solutions, 77 K)

Compound		$E(^*π←π)$ transitions		$E(^1ππ^*)$	$E(^3ππ^*)$	$\tau(^3ππ^*)/\text{ms}$
B_6bL^6		37880 (3.66)	36900 (3.66)	33080	22870	83 ± 4
La	1 : 1	37170 (3.56)	36130 (3.54)	31230	20350	93 ± 4
Eu	1 : 1	37170 (3.31)	36130 (3.29)	^b	^b	^b
Gd	1 : 1	37040 (3.56)	36000 (3.54)	32790	21630	^c
Tb	1 : 1	37040 (3.41)	36050 (3.39)	^b	^b	^b
La	1 : 2	37040 (3.84)	36170 (3.83)	32250	21070	150 ± 5
Eu	1 : 2	37040 (3.87)	36190 (3.86)	^b	^b	^b
Gd	1 : 2	36900 (3.84)	36010 (3.83)	33000	23680	^c
Tb	1 : 2	36900 (3.75)	35990 (3.74)	^b	(21000) ^d	^b

^a Maximum of the band envelope; molar absorption coefficients ($\log \epsilon$) are given within parentheses. ^b Not detected due to energy transfer on the metal ion. ^c Not measured. ^d Interferes with metal-centred luminescence.

Table 5 Absolute quantum yields (Q_{abs}) and lifetimes (τ) of the metal-centred luminescence upon ligand excitation of complexes ($1.5\text{--}2.5 \times 10^{-5}$ M) in dry and degassed acetonitrile ($\tilde{\nu}_{\text{exc}} \approx 35900 \text{ cm}^{-1}$) and in the solid state ($\tilde{\nu}_{\text{exc}} = 32470 \text{ cm}^{-1}$)

Compound	Exptl. conditions ^a	τ/ms	$Q_{\text{abs}}(\%)$
Eu, 1 : 1 (2)	SS, 20 K	0.34 ± 0.01 (86%)	1.5 \pm 0.3
	SS, 295 K	1.36 ± 0.09 (14%)	
	Sol	0.34 ± 0.01	
Eu, 1 : 2 (6)	SS, 20 K	1.54 ± 0.06	2.5 \pm 0.5
	SS, 295 K	0.51 ± 0.01	
	Sol	0.43 ± 0.01	
Tb, 1 : 1 (4)	SS, 10 K	2.00 ± 0.06	4.8 \pm 1.0
	SS, 295 K	1.31 ± 0.01 (76%)	
	Sol	3.1 ± 0.1 (24%)	
Tb, 1 : 2 (8)	SS, 20 K	1.26 ± 0.01	1.6 \pm 0.3
	SS, 295 K	2.06 ± 0.06	
	Sol	2.13 ± 0.02	
	Sol	2.25 ± 0.07	

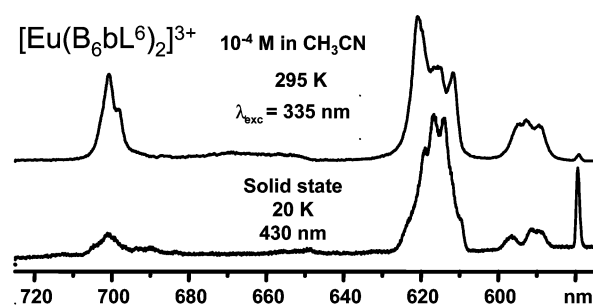
^a Key: SS = solid state, Sol = solution in acetonitrile at 295 K.

transition occurs at 17262 (1 : 1 complex) and 17260 cm^{-1} (1 : 2 complex). It is broad (full width at half height, $\text{fwhm} = 34$ and 29 cm^{-1} , respectively), asymmetric and unusually intense. These data point to a statistical distribution of similar Eu(III) ion sites with low symmetry, possibly C_{2v} or C_2 in view of the intensity of the 0–0 transition.²⁹ The excitation spectra in the $^5D_0 \leftarrow ^7F_0$ range confirm these results while revealing a broad shoulder at 17292 cm^{-1} in the case of the 1 : 1 complex. Direct excitation of the 5D_0 level results in more resolved spectra and confirms the maximum splitting of the ligand field levels. For instance, identified 7F_1 sublevels occur at 265, 360 and 501 cm^{-1} in the 1 : 1 complex and at 281, 367 and 509 cm^{-1} in the 1 : 2 complex, in line with a low site symmetry. The $^5D_0 \rightarrow ^7F_2$ transition is more difficult to analyse because of the interaction of the electronic sub-levels with the phonon density of states. Identified vibronic transitions occur at 919, 932 and 1095 cm^{-1} (1 : 1 complex) or 839, 966 and 1149 cm^{-1} (1 : 2 complex).

The luminescent decay of the $\text{Eu}(^5D_0)$ level is found to be bi-exponential at 20 K for the 1 : 1 complex, with a short lifetime (τ , Table 5) reflecting the presence of at least two (possibly three) water molecules in the inner coordination sphere and a longer lifetime corresponding to an environment with zero (possibly one) water molecule, as has been observed for the complexes with B_4bL^4 .¹² For the 1 : 2 complex, a single exponential is seen with a short lifetime, reflecting the presence of efficient deactivation processes. A similar situation occurs for the Tb(III) compounds (Fig. S6, ESI†, Table 5). For the 1 : 1 complex, the short lifetime corresponds to the coordination of about two water molecules in the inner sphere while the longer lifetime is typical of an environment containing between 0 and 1 water molecules²⁹ (lifetimes up to 7.25 ms have been reported for the corresponding complex with B_4bL^4).¹² It is noteworthy

that the lifetime of the Tb 1 : 2 complex, which also reflects a metal ion environment with a maximum of one water molecule, is independent of the temperature in the range 20–295 K while that of the 1 : 1 complex decreases dramatically upon increasing the temperature to 295 K. In addition to quenching by high energy vibrations, the 5D_J levels may also be deactivated by temperature-dependent processes, ligand-to-metal charge transfer (LMCT) states for Eu and back transfer processes for Tb.³⁰ In our case, the energy differences between the metal ion excited state and the ligand triplet state (taken as the values for the Gd complexes) amount to 4400 (1 : 1) and 6430 (1 : 2) cm^{-1} for the Eu complexes and to 1210 (1 : 1) and 3260 (1 : 2) cm^{-1} for the Tb complexes. From these data, it is clear that sizeable $^3ππ^* \leftarrow ^5D_4$ back transfer may occur for the Tb 1 : 1 complex, but not for the 1 : 2 compound, henceforth the different dependence of the lifetimes with temperature. The situation for the Eu complexes is more difficult to explain, especially that no LMCT could be evidenced on the absorbance spectra. One notes, however, that intermolecular interactions may occur in the solid state, leading to additional deactivation paths.

The situation is quite different for solutions in acetonitrile. All the luminescence decays are single exponentials and the associated lifetimes are long (Table 5), reflecting the presence of molecular species with at most one water molecule coordinated onto the metal ion, in line with the NMR data (see above). Therefore some structural changes occur in going from the solid state to solution, as exemplified by the emission spectrum of the Eu 1 : 2 complex (Fig. 6): compared with the solid state data, the

**Fig. 6** Luminescence spectra of $[\text{Eu}(\text{B}_6\text{bL}^6)_2]^{3+}$ (6) as a solid state sample (bottom) and in acetonitrile solution (top). Vertical scale: arbitrary units.

0–0 transition has a much lower intensity and the splitting pattern of the 7F_1 level is quite different. Quantum yields (Table 5) are sizeable given the fact that no specially designed antenna group has been grafted onto B_6bL^6 . They are somewhat larger than the ones reported for the corresponding complexes with B_4bL^4 : 2.6 and 0.3% for the 1 : 1 and 1 : 2 Tb complexes, and 0.05–0.07% for the Eu complexes.¹²

Conclusion

NMR studies confirm that the *p*-*tert*-butylcalix[6]arene B_6bL^6 adopts a semi-mobile structure with a distorted alternate *in-out* conformation at elevated temperatures in dmsO and CH_2Cl_2 solutions. At 405 K in dmsO- d_6 , the averaged structure possesses C_{6v} symmetry. Molecular modelling calculations confirm that the structure observed in the solid state, in which phosphoryl groups interact with water molecules, is a good model for the solution structure, which may explain the formation of a colloidal phase in water- CH_2Cl_2 during the work up of the ligand with water. The stability constants for the complexes with La(III) are somewhat smaller (1 : 1 complex) or equal (1 : 2) to the ones found for the corresponding *p*-*tert*-butylcalix[4]arene,¹² probably in view of the larger flexibility of the calix[6]arene macrocycle. On the other hand, photophysical properties are enhanced with respect to the smaller calix[4]arene, which opens the way to sensitive luminescence detection of these complexes, a definite advantage for quantifying extraction processes. Work is in progress in our laboratories to investigate the structure of the 1 : 2 complexes and to assess the extraction capability of B_6bL^6 .

Experimental

Syntheses and characterisations

Solvents and starting materials were purchased from Fluka AG (Buchs, Switzerland) and Acros; chloro(dimethylphosphinoyl)methane from Hoechst AG; *p*-*tert*-butylcalix[6]arene was synthesised according to the procedure reported in the literature.³¹ With the exception of the last two compounds, they were used without further purification unless otherwise stated. Toluene was distilled over Na and acetonitrile over CaH_2 . Lanthanide perchlorates were prepared from the oxides (Rhône-Poulenc, 99.99%) and their metal content determined by titration with Titriplex III (Merck) in the presence of urotropine and xylene orange.³² Elemental analyses were performed by Dr H. Eder (Microchemical Laboratory), University of Geneva, Switzerland.

Synthesis of B_6bL^6 . A warm solution of chloro(dimethylphosphinoyl)methane (1.85 g, 14.62 mmol) in toluene (30 cm³) was added to the refluxing fine suspension of the hexasodium derivative of *p*-*tert*-butylcalix[6]arene in toluene. The latter was prepared by addition of sodium (0.34 g, 14.63 mmol) to a mixture of *p*-*tert*-butylcalix[6]arene (2.03 g, 2.09 mmol), methanol (50 cm³) and toluene (150 cm³), followed by distillation of the methanol and a part of the toluene. The resulting mixture was refluxed with stirring under nitrogen for 90 h. After cooling to 50–60 °C the mother liquor was separated by filtration, the precipitate was washed with three portions (50 cm³ each) of warm (323 K) toluene and mixed with methylene chloride (120 cm³). Sodium chloride was separated by filtration and 1 M HCl aqueous solution (80 cm³) was added. The mixture was stirred for 15 min at room temperature. A white thick phase formed between the water and methylene chloride layers. It was separated by centrifugation and washed with water; the process was repeated until negative reaction for chloride was obtained (the pH of the water portions became neutral). The residue was dissolved in methanol (30 cm³) and after filtration the solvent was evaporated. The crude product was recrystallised from a methylene chloride–hexane mixture and a white husk-like powder product was isolated (1.35 g, 43%). $R_f = 0.27$, $CH_2Cl_2 : CH_3OH : 25\% NH_3 : 4 : 10 : 3$ v/v; mp 330–335 °C (decomp.). Found: C, 63.87; H, 8.96; P, 11.32. Calc. for $C_{84}H_{134}O_{16}P_6$ ($B_6bL^6 \cdot 4H_2O$): C, 63.62; H, 8.52; P, 11.72%. IR: $\nu(P=O)$ 1178 cm⁻¹ (KBr disk, after heating for 24 h at 393 K). ¹H NMR (400 MHz, dmsO- d_6 , 405 K): δ 7.13 (12 H, s, Ar-H), 4.09 (12 H, s, Ar-CH₂-Ar), 3.92 (12 H, bs, CH₂-P=O), 1.30 [36 H, d, ²J_{HP} = 4.92 Hz, (CH₃)₂P=O], 1.15 [54 H, s,

$(CH_3)_3$]. ³¹P{¹H} NMR (161.9 MHz, dmsO- d_6 , 378 K): +35.82 (s). ¹²C{¹H} NMR (400 MHz, dmsO- d_6 , 378 K): δ 146.1 (C⁵), 133.1 (C^{3,7}), 34.5 [C(CH₃)₃], 31.5 [C(CH₃)₃]. ¹²C{¹H} NMR (400 MHz, CDCl₃, 293 K): δ 152.1 (C⁸), 146.5 (C⁵), 131.5 (C^{3,7}), 128.5, 125.5 (C^{4,6}), 72.5, 71.5 (CH₂P), 34.5 [C(CH₃)₃], 32.1 [C(CH₃)₃], 29.6 (C²), 17.5, 17.0 [(CH₃)₂P]. ES-MS (MeOH-CH₃CO₂H), $m/z = 1513.6$ (B_6bL^6) and 1535.5 ($B_6bL^6 + Na$)⁺. The substituted *p*-*tert*-butylcalix[6]arene is soluble at room temperature in several organic solvents such as methanol, ethanol, isopropanol, acetonitrile, methylene chloride, chloroform, dimethylformamide, dimethyl sulfoxide and glacial acetic acid. It is sparingly soluble, even at higher temperatures, in acetone, tetrahydrofuran, dioxane, toluene, xylene, ethyl acetate, and nitromethane, and is insoluble in aliphatic hydrocarbons, tetrachloromethane, dimethyl ether, diisopropyl ether, and water. It can be re-crystallised from various solvents and solvent mixtures: toluene, xylene, dimethoxyethane, ethanol–water, acetonitrile–diisopropyl ether, chloroform–diisopropyl ether, acetone–*n*-hexane, ethyl acetate–*n*-hexane, chloroform–*n*-hexane, methylene chloride–hexane.

1 : 1 Complexes. A solution of $Ln(ClO_4)_3 \cdot xH_2O$ (0.1 mmol, Ln = La, Eu, Tb and Gd) in 2 cm³ EtOH was heated at 43 °C and 0.1 mmol B_6bL^6 in 4 cm³ EtOH was added dropwise. A precipitate appeared and the mixture was stirred for 5 h under an N₂ atmosphere at rt. The precipitate was centrifuged, washed three times with 8 cm³ EtOH and dried for 12 h at 313 K and for 24 h at 348 K under vacuum at 10⁻² torr. The La compound appeared as brilliant greenish-yellow microcrystals while the others were slightly yellow powders. No suitable single crystals for X-ray analysis could be obtained. Yields: 64 (La), 62 (Eu), 44 (Gd), 39% (Tb). Found: C, 50.09; H, 6.89. Calc. for $La(B_6bL^6)(ClO_4)_3 \cdot 3H_2O$: C, 50.37; H, 6.54%. Elemental analyses for the other complexes did not yield satisfactorily results due to their hygroscopic nature. High-resolution FAB-MS: $[La(B_6bL^6)]^{3+}$ $m/z = 550.89$ (calc. 550.89); $[Eu(B_6bL^6)]^{3+}$ $m/z = 555.23$ (calc. 555.25); $[Gd(B_6bL^6)]^{3+}$ $m/z = 556.89$ (calc. 557.01); experimental isotopic distribution patterns matched the calculated ones. IR: $\nu(P=O)$ 1180, shift 7, 7, 11, and 7 cm⁻¹ for La, Eu, Gd and Tb, respectively; (KBr disk, after heating for 24 h at 393 K) 1120, 1004 (La), 1024 (Eu, Gd, Tb) (–O–CH₂–); $\nu(ClO_4)$ 1087–1105, 625–629 cm⁻¹; Ln–O (361 La, 364 Eu, 363 Gd).

1 : 2 Complexes. A solution of $Ln(ClO_4)_3 \cdot xH_2O$ (0.06 mmol, Ln = La, Eu, Tb and Gd) in 6 cm³ of dry CH₃CN was added dropwise to a solution of 0.1 mmol B_6bL^6 in 25 cm³ of dry CH₃CN heated at 318 K. The resulting mixture was stirred for 5 h under an N₂ atmosphere at 318 K and for one additional hour without heating. The solvent was half evaporated and replaced by diisopropyl ether until the solution turned turbid (45 cm³). The precipitate was centrifuged, washed with diisopropyl ether and dried for 12 h at 313 K and for 24 h at 348 K under vacuum at 10⁻² torr. The four compounds were slightly yellow powders. Yields: 72 (La), 50 (Eu), 44 (Gd), 38% (Tb). The compounds are hygroscopic, although less than the 1 : 1 complexes. Found: C, 56.79; H, 7.95. Calc. for $La(B_6bL^6)_2(ClO_4)_3 \cdot 3H_2O$: C, 57.34; H, 7.39%. Found: C, 56.79; 7.84. Calc. for $Eu(B_6bL^6)_2(ClO_4)_3 \cdot 3H_2O$: C, 57.13; H, 7.36%. Found: C, 56.47; 7.77. Calc. for $Gd(B_6bL^6)_2(ClO_4)_3 \cdot 5H_2O$: C, 56.46; H, 7.40%. Found: C, 55.50; 7.69. Calc. for $Tb(B_6bL^6)_2(ClO_4)_3 \cdot 4H_2O$: C, 57.02; H, 7.35%. High-resolution FAB-MS: $[La(B_6bL^6)_2(H_2O)]^{3+}$ $m/z = 1061.46$ (calc. 1061.47); $[Eu(B_6bL^6)_2]^{3+}$ $m/z = 1059.49$ (calc. 1059.48); $[Gd(B_6bL^6)_2]^{3+}$ $m/z = 1061.15$ (calc. 1061.15); $[Tb(B_6bL^6)_2]^{3+}$ $m/z = 1061.49$ (calc. 1061.49); experimental isotopic distribution patterns matched the calculated ones. IR: $\nu(P=O)$ 1180 shift 11, 10, 4, and 6 cm⁻¹ for La, Eu, Gd and Tb, respectively; (KBr disk, after heating for 24 h at 120 °C) 1120 (R₃P=O), 1023–1020 (–O–CH₂–); $\nu(ClO_4)$ 1097–1109, 624–626 cm⁻¹.

Table 6 Selected experimental parameters for the crystal structure determination of the hexa-dimethylphosphinoylmethoxy-*p*-*tert*-butyl-calix[6]arene

Empirical formula	C ₈₄ H ₁₂₆ O ₁₂ P ₆ ·13H ₂ O·0.5C ₇ H ₈
Formula weight	1793.94
Crystal system	Monoclinic
Space group	<i>P</i> 2 ₁ / <i>c</i>
<i>a</i> /Å	25.552(11)
<i>b</i> /Å	30.500(14)
<i>c</i> /Å	27.111(3)
β /°	104.88(3)
<i>V</i> /Å ³	20419(13)
<i>Z</i>	8
μ /mm ⁻¹	0.171
<i>T</i> /K	143(2)
<i>F</i> (000)	7768
Reflections measured	104 975
Independent reflections	31 919 (<i>R</i> _{int} = 0.1938)
<i>R</i> 1 [<i>I</i> > 2 σ (<i>I</i>)], <i>wR</i> 2 (all data)	0.1035, 0.3378

Crystal structure determination of B₆bL⁶

Brilliant white crystals of the *p*-*tert*-calix[6]arene derivative were obtained as follows: a 0.002 M solution of the ligand in dry CH₃CN was partly evaporated at room temperature. When the total volume was reduced to 25%, the flask was placed inside a bigger flask containing 5 cm³ of a 1 : 1 (v/v) mixture of toluene–acetonitrile and kept in a refrigerator for two weeks. Diffraction data were collected at 143 K on a 0.13 × 0.10 × 0.07 mm crystal with the help of a mar345 imaging plate diffractometer. Data reduction was performed with marHKL release 1.9.1.³³ The structure was solved with *ab initio* direct methods.³⁴ The structure was refined using the full-matrix-block least-squares on *F*² with all non-H atoms (toluene solvent and water molecules were excluded) anisotropically defined. H atoms were placed in calculated positions using the «riding model» with *U*_{iso} = *a***U*_{eq}(X) where *a* is 1.5 for methyl hydrogen protons and 1.2 for others, and X is the parent carbon atom. No hydrogen atoms were located for the water molecules. Owing to the poor quality of data as a result of disordered and diffuse solvent and water molecules, anti-bumping restraints in combination with SWAT³⁵ [*g* = 0.285(5); *U* = 0.30(1)] have been employed in order to handle this problem during the refinement. Structure refinement, molecular graphics and geometrical calculation have been carried out using the SHELXTL software package, release 5.1.³⁵ Experimental details are listed in Table 6.

CCDC reference number 188700.

See <http://www.rsc.org/suppdata/dt/b2/b206238k/> for crystallographic data in CIF or other electronic format.

Molecular modelling

The calculations were done in a Silicon Graphics work-station using the Cerius2 version 3.8 package developed by Molecular Simulations Incorporated. All the geometrical optimisations were done without constraint. Universal 1.02 and Dreiding force fields were used. The energy minimization was performed until the energy gradient was lower than 0.01 kcal mol⁻¹. Between each set of energy minimizations, the calixarene was heated with a molecular dynamics simulation to analyse the energy surface and obtain the lowest energy structure.

Physicochemical measurements

The IR spectra were measured on a Mattson Alpha Centauri FT spectrometer as KBr pellets. The ES-MS spectrum of the ligand was measured on a Finnigan SSQ 710C spectrometer driven by a Digital Personal station 5000/25 on approx. 10⁻⁴ M solution in methanol and MeOH–CH₃CO₂H as eluent. High resolution MS-FAB spectra were recorded on an FTMS 4.7T BioApex II spectrometer from Bruker by the MS-Service unit of the University of Fribourg (Switzerland). NMR spectra

were recorded on Bruker DRX Avance 400 or AM-360 (360.16 MHz) spectrometers; ¹H: δ /ppm with reference to TMS or related to the residual peak of the degassed and dried CD₃CN; ³¹P{¹H}: δ /ppm with reference to H₃PO₄ 85% as external reference. Spectrophotometric titrations were performed at 298 K on a UV-Vis Perkin-Elmer Lambda 7 PC-controlled spectrometer with 1 cm quartz cells. In a typical experiment, 7 cm³ of a 1.7 × 10⁻⁴ M solution of B₆bL⁶ in dry and degassed spectrophotometric grade acetonitrile were titrated in the glove-box by increasing the amount of a 2.4 × 10⁻⁴ M solution of lanthanum perchlorate delivered by a 1 cm³ micropipette; 30 spectra were recorded for Ln : L ratios between 0 and 4 : 1 and fitted using the SPECFIT program.³⁶ Low resolution luminescence spectra and lifetimes (at least five determinations), were recorded on a Perkin-Elmer LS-50B spectrofluorimeter at 295 and 77 K. High resolution laser excited luminescence spectra and lifetimes have been measured at variable temperature using published procedures.³⁷ The quantum yields of the metal-centred luminescence were determined using published procedures in degassed and anhydrous CH₃CN at room temperature with respect to complexes with a cyclen derivative, [EuL]³⁺ and [TbL]³⁺ 3 × 10⁻⁵ M in water (*Q*_{abs} = 23.1 and 25.4%, respectively) (L = 1,3,7,10-tetrakis[*N*-(4-phenylacetyl)carbamoylmethyl-1,4,7,10-tetraazacyclododecane]).³⁸ The refractive indexes were 1.344 for solutions in CH₃CN and 1.333 for solutions in water, the excitation wavelengths 279 (Eu, absorbance 0.50) and 278 (Tb, absorbance 0.37) nm; a filter (430 nm) was inserted to eliminate the Raleigh diffusion band and second order spectra.

Acknowledgements

We thank Ms Véronique Foiret for her technical assistance in luminescence measurements, Mr Daniel Baumann for infrared measurements and David Kony (University of Geneva) for his help in the molecular mechanics calculations. This work is supported through grants from the Swiss National Science Foundation (project SCOPES 7BUPJ062293), the Herbette Foundation (Lausanne) and the National Institute of Nuclear Research of México.

References

- (a) *Calixarenes 2001*, Z. Asfari, V. Böhmer, J. M. Harrowfield and J. Vicens, ed., Kluwer Academic Publishers, Dordrecht, 2001; (b) *Calixarenes for Separations*, G. J. Lumetta, R. D. Rogers and A. Gopalan, ed., ACS Symposium Series 757, American Chemical Society, Washington D.C., 2000; (c) L. Mandolini and R. Ungaro, *Calixarenes in Action*, Imperial College Press, London, 2000; (d) C. D. Gutsche, *Calixarenes Revisited*, The Royal Society of Chemistry, Cambridge, 1998; (e) C. D. Gutsche, *Calixarenes*, The Royal Society of Chemistry, Cambridge, 1989.
- G. G. Talanova, *Ind. Eng. Chem. Res.*, 2000, **39**, 3550; S. D. Alexandratos and S. Natesan, *Ind. Eng. Chem. Res.*, 2000, **39**, 3998; A. Kononov, I. Antipin, A. Burilov, E. Kazakova, A. Mustafina and M. Punovik, *Phosphorus Sulfur Silicon Relat. Elem.*, 1999, **146**, 701; C. Wieser-Jeunesse, D. Matt, M. R. Yafitian, M. Burgard and J. M. Harrowfield, *C. R. Acad. Sci., Ser. IIC*, 1998, **1**, 479.
- F. Cadogan, K. Nolan and D. Diamond, in *Calixarenes 2001*, Z. Asfari, V. Böhmer, J. M. Harrowfield and J. Vicens, ed., Kluwer Academic Publishers, Dordrecht, 2001, p. 627.
- R. Paciello, L. Siggel and M. Roper, *Angew. Chem., Int. Ed.*, 1999, **38**, 1920.
- F. Cadogan, P. Kane, M. A. McKervey and D. Diamond, *Anal. Chem.*, 1999, **71**, 5544.
- F. Arnau-Neu, J. K. Browne, D. Byrne, D. J. Marrs, M. A. McKervey, P. O'Hagan, M.-J. Schwing-Weill and A. Walker, *Chem. Eur. J.*, 1999, **5**, 175; J.-F. Dozol, H. Rouquette, V. Böhmer, C. Grüttner, R. A. Jakobi, D. Kraft and W. Vogt, *Fr. pat.*, 01158E, 1995; F. Arnau-Neu, V. Böhmer, J.-F. Dozol, C. Grüttner, R. A. Jakobi, D. Kraft, O. Mauprivez, H. Rouquette, M.-J. Schwing-Weill, N. Simon and W. Vogt, *J. Chem. Soc., Perkin Trans. 2*, 1996, 1175.

- 7 G. R. Choppin, Report DE97005235, DOE, Office for Energy Research, USA, 1997.
- 8 J. F. Malone, D. J. Marrs, M. A. McKervey, P. O'Hagan, N. Thompson, A. Walker, F. Arnaud-Neu, O. Maurivez, M. J. Schwing-Weill, J.-F. Dozol, H. Rouquette and N. Simon, *J. Chem. Soc., Chem. Commun.*, 1995, 2151.
- 9 F. Arnaud-Neu, S. Barbosa, D. Byrne, L. J. Charbonnière, M.-J. Schwing-Weill and G. Ulrich, in *Calixarenes for Separations*, G. J. Lumetta, R. D. Rogers and A. Gopalan, ed., ACS Symp. Ser. 757, American Chemical Society, Washington D.C., 2000, ch. 12, p. 150ff; B. Lambert, V. Jacques, A. Shivanyuk, S. E. Matthews, A. Tunayar, M. Baaden, G. Wipff, V. Böhmer and J. F. Desreux, *Inorg. Chem.*, 2000, **39**, 2033; F. Arnaud-Neu, J. K. Browne, D. Byrne, D. J. Marrs, M. A. McKervey, P. O'Hagan, M. J. Schwing-Weill and A. Walker, *Chem. Eur. J.*, 1999, **5**, 175; S. Barbosa, A. Garcia Carrera, S. E. Matthews, F. Arnaud-Neu, V. Böhmer, J.-F. Dozol, H. Rouquette and M.-J. Schwing-Weill, *J. Chem. Soc., Perkin Trans. 2*, 1999, 719.
- 10 J.-C. G. Bünzli, F. Besançon and F. Ihringer, in *Calixarenes for Separations*, G. J. Lumetta, R. D. Rogers and A. Gopalan, ed., ACS Symp. Ser. 757, American Chemical Society, Washington D.C., 2000, ch. 14, p. 179ff.
- 11 F. de M. Ramirez, L. Charbonnière, G. Muller, R. Scopelliti and J.-C. G. Bünzli, *J. Chem. Soc., Dalton Trans.*, 2001, 3205.
- 12 L. Le Saulnier, S. Varbanov, R. Scopelliti, M. Elhabiri and J.-C. G. Bünzli, *J. Chem. Soc., Dalton Trans.*, 1999, 3919.
- 13 Y. Rondelez, M.-N. Ragher, A. Duprat and O. Reinaud, *J. Am. Chem. Soc.*, 2002, **124**, 1334.
- 14 D. E. Corbridge, in *The Infrared Spectra of Phosphorus Compounds, Topics in Phosphorus Chemistry*, D. M. Grayson and E. J. Griffith, ed., John Wiley and Sons, New York-Toronto, 1969, vol. 6, pp. 235–365.
- 15 F. de M. Ramirez, S. Varbanov, L. J. Charbonnière, C. Cécile, R. Scopelliti, and J.-C. G. Bünzli, unpublished results.
- 16 M. M. Mark, C. H. Dungan, M. M. Grutchfield and J. R. van Wazer, in *Topics in Phosphorus Chemistry, Compilation of ³¹P NMR Data*, M. Grayson and E. J. Griffith, ed., John Wiley & Sons, New York, 1967, vol. 5, pp. 227–475; E. N. Tsvetkov, T. E. Kron and M. I. Kabachnik, *Izv. Akad. Nauk SSSR, Ser. Khim.*, 1980, **3**, 669.
- 17 H. E. Gottlieb, V. Kotlyar and A. Nudelman, *J. Org. Chem.*, 1997, **62**, 7512; D. H. Williams and I. Fleming, *Spectroscopic Methods in Organic Chemistry*, McGraw-Hill Book Company (UK), Ltd., London, 3rd edn., 1980, ch. 3, p. 75ff.
- 18 R. G. Janssen, J. P. M. van Duynhoven, W. Verboom, G. J. van Hummel, S. Harkema and D. N. Reinhoudt, *J. Am. Chem. Soc.*, 1996, **118**, 3666.
- 19 S. Kanamathareddy and C. D. Gutsche, *J. Org. Chem.*, 1994, **59**, 3871.
- 20 R. Ungaro, A. Pochini, G. D. Andreotti and P. Domiano, *J. Inclusion Phenom.*, 1985, **3**, 35.
- 21 J. Sandstöm, *Dynamic NMR Spectroscopy*, Academic Press, London, 1982.
- 22 J. O. Magrans, A. M. Rincón, F. Cuevas, J. López-Prados, P. M. Nieto, M. Pons, P. Prados and J. M. Mendoza, *J. Org. Chem.*, 1998, **63**, 1079.
- 23 T. Harada and S. Shinkai, *J. Chem. Soc., Perkin Trans 2*, 1995, 2231.
- 24 M. Halit, D. Owler, M. Perrin, A. Thozet, R. Perrin, J. Vicens and M. Bourakhoudar, *J. Inclusion Phenom. Macrocycl. Chem.*, 1988, **6**, 613; W. P. van Hoorn, F. C. J. M. van Veggel and D. N. Reinhoudt, *J. Org. Chem.*, 1996, **61**, 7180.
- 25 M. A. Molins, P. M. Nieto, C. Sanchez, P. Prados, J. de Mendoza and M. Pons, *J. Org. Chem.*, 1992, **57**, 6924; C. Gutsche and L. J. Bauer, *J. Am. Chem. Soc.*, 1985, **107**, 6052.
- 26 P. Neri, C. Rocco, G. M. L. Consoli and M. Piattelli, *J. Org. Chem.*, 1993, **58**, 6535.
- 27 K. Nakamoto, *Infrared and Raman Spectra of Inorganic and Coordination Compounds. Part A. Theory and Applications in Inorganic Chemistry*, John Wiley Interscience Publ., New York, 1997; J.-C. G. Bünzli, J.-R. Yersin and C. Mabillard, *Inorg. Chem.*, 1983, **21**, 1471; G. Muller, J.-C. G. Bünzli, K. J. Schenk, C. Piguet and G. Hopfgartner, *Inorg. Chem.*, 2001, **40**, 2642.
- 28 M. Latva, H. Takalo, V. M. Mikkala, C. Matescu, J.-C. Rodriguez-Ubis and J. Kankare, *J. Lumin.*, 1997, **75**, 149.
- 29 J.-C. G. Bünzli, in *Lanthanide Probes in Life, Chemical and Earth Sciences, Theory and Practice*, J.-C. G. Bünzli and G. R. Choppin, ed., Elsevier Science Publ. B.V., Amsterdam, 1989, ch. 7, p. 219.
- 30 J.-C. G. Bünzli and C. Piguet, in *Encyclopedia of Materials: Science and Technology*, K. H. J. Buschow, R. W. Cahn, M. C. Fleming, B. Ilshner, E. J. Kramer and S. Mahajan, ed., Elsevier Science Ltd, Oxford, 2001, vol. 10, p. 4465.
- 31 C. D. Gutsche, B. Dhawan, M. Leonis and D. Stewart, *Org. Synth.*, 1990, **68**, 238.
- 32 G. Schwarzenbach, *Complexometric Titrations*, Chapman & Hall, London, 1957.
- 33 Z. Otwinowski and W. Minor, *Macromolecular Crystallography, Part A*, C. W. Jr. Carter and R. M. Sweet, ed., Academic Press, New York, 1997, pp. 307–326.
- 34 G. M. Sheldrick, *Acta Crystallogr., Sect. A*, 1990, **46**, 467.
- 35 SHELXTL, version 5.1.0., G. M. Sheldrick, University of Göttingen, Germany, 1997; Bruker AXS Inc., Madison, Wisconsin, USA, 1997.
- 36 H. Gampp, M. Maeder, C. J. Meyer and A.D. Zuberbühler, *Talanta*, 1985, **32**, 257.
- 37 J.-C. G. Bünzli and A. Milicic-Tang, *Inorg. Chim. Acta*, 1996, **252**, 221.
- 38 G. Zucchi, A.-C. Ferrand, R. Scopelliti and J.-C. G. Bünzli, *Inorg. Chem.*, 2002, **41**, 2459.